Generation of μJ multicolor femtosecond laser pulses using cascaded four-wave mixing

Jun Liu [1, 2,*], and Takayoshi Kobayashi [1, 2, 3, 4]

1Department of Applied Physics and Chemistry and Institute for Laser Science, University of Electro-Communications, Chofugaoka 1-5-1, Chofu, Tokyo 182-8585 Japan
2 International Cooperative Research Project (ICORP), Japan Science and Technology Agency, 4-1-8 Honcho, Kawaguchi, Saitama 332-0012, Japan
3Department of Electrophysics, National Chiao Tung University, 1001 Ta Hsueh Rd. Hsinchu 300, Taiwan
4 Institute of Laser Engineering, Osaka University, Yamadakami 2-6, Suita 565-0871, Ibaraki 567-0047, Japan
**Corresponding author: jliu@ils.uec.ac.jp.*

Abstract: Multicolor femtosecond pulses were simultaneously obtained by a cascaded FWM process in fused silica glass. The sideband spectra were tunable by changing the crossing angle of the two input beams. Frequency up-shift and down-shift pulses with energies as high as 1 μJ, durations of 45 fs, nearly diffraction limited Gaussian spatial profiles, and power stability smaller than 2% RMS of the generated sidebands were obtained. These multicolor sidebands can be used in various experiments, such as multicolor pump-probe experiment.

OCIS codes: (190.4380) Nonlinear optics, four-wave-mixing; (320, 2250) Femtosecond phenomena; (190, 7110) Ultrafast nonlinear optics.

References and links

1. T. Kobayashi, A. Shirakawa, and T. Fuji, "Sub-5-fs transform-limited visible pulse source and its application to real-time spectroscopy," IEEE J. Sel. Top. Quantum Electron. **7,** 525-538 (2001).
2. A. Baltuška, T. Fuji, and T. Kobayashi, "Visible pulse compression to 4 fs by optical parametric amplification and programmable dispersion control," Opt. Lett. **27**, 306-308 (2002).
3. G. Cerullo and S. De Silvestri, "Ultrafast optical parametric amplifiers," Rev. Sci. Inst. **74**, 1-18 (2003).
4. H. Crespo, J. T. Mendonça, and A. Dos Santos, "Cascaded highly nondegenerate four-wave-mixing phenomenon in transparent isotropic condensed media," Opt. Lett. **25**, 829-831 (2000).
5. L. Misoguti, S. Backus, C. G. Durfee, R. Bartels, M. M. Murnane, and H. C. Kapteyn, "Generation of broadband VUV light using third-order cascaded processes," Phys. Rev. Lett. **87**, 013601(2001).
6. F. Th´eberge, N. Ak¨ozbek, W. Liu, A. Becker, and S. L. Chin, "Tunable ultrashort laser pulses generated through filamentation in gases," Phys. Rev. Lett. **97**, 023904 (2006).
7. T. Fuji, T. Horio, and T. Suzuki, "Generation of 12 fs deep-ultraviolet pulses by four-wave mixing through filamentation in neon gas," Opt. Lett. **32**, 2481-2483 (2007).
8. T. Fuji and T. Suzuki, "Generation of sub-two-cycle mid-infrared pulses by four-wave mixing through filamentation in air," Opt. Lett. **32**, 3330-3332 (2007).
9. A. Dubietis, G. Tamošauskas, P. Polesana, G. Valiulis, H. Valtna, D. Faccio, P. Di Trapani, and A. Piskarskas, "Highly efficient four-wave parametric amplification in transparent bulk Kerr medium," Opt. Express **15**, 11126-11132 (2007), http://www.opticsinfobase.org/abstract.cfm?URI=oe-15-18-11126.
10. M. Zhi and A. V. Sokolov, "Broadband coherent light generation in a Raman-active crystal driven by two-color femtosecond laser pulses," Opt. Lett. **32**, 2251-2253 (2007).
11. J. Liu, J. Zhang, and T. Kobayashi, "Broadband coherent anti-Stokes Raman scattering light generation in BBO crystal by using two crossing femtosecond laser pulses," Opt. Lett. **33**, 1494-1496 (2008).
12. H. Valtna, G. Tamošauskas, A. Dubietis, and A. Piskarskas, "High-energy broadband four-wave optical parametric amplification in bulk fused silica," Opt. Lett. **33**, 971-973 (2008).
13. H. Crespo and R. Weigand, "Cascaded four-wave mixing technique for high-power few-cycle pulse generation," in *XVI International Conference on Ultrafast Phenomena*, (UP, 2008) paper frilp-5.
14. J. Liu, and T. Kobayashi, "Cascaded four-wave mixing and multicolored arrays generation in a sapphire plate by using two crossing beams of femtosecond laser," Opt. Express **16,** 22119-22125 (2008).
15. J. Liu and T. Kobayashi, "Wavelength-tunable multicolored femtosecond laser pulses generation in a fused silica glas," (submitted).

#105514 - $15.00 USD Received 18 Dec 2008; revised 2 Feb 2009; accepted 23 Feb 2009; published 16 Mar 2009

16. D. Pestov, R. K. Murawski, G. O. Ariunbold, X. Wang, M. C. Zhi, A. V. Sokolov, V. A. Sautenkov, Y. V. Rostovtsev, A. Dogariu, Y. Huang, and M. O. Scully, "Optimizing the laser-pulse configuration for coherent Raman spectroscopy," Science **316,** 265-268(2007).
17. R. M. Hochstrasser, "Two-dimensional spectroscopy at infrared and optical frequencies," PNAS 104, 14190-14196 (2007).
18. R. Zgadzaj, E. Gaul, N. H. Matlis, G. Shvets, and M. C. Downer, "Femtosecond pump-probe study of preformed plasma channels," J. Opt. Soc. Am. B **21,** 1559-1567 (2004).
19. P. B. Lundquist, D. R. Andersen, and Y. S. Kivshar, "Multicolor solitons due to four-wave mixing," Phys. Rev. E **57**, 3551–3555 (1998).
20. G. Fanjoux, J. Michaud, M. Delqu´e, H. Mailotte, and T. Sylvestre, "Generation of multicolor vector Kerr solitons by cross-phase modulation, four-wave mixing, and stimulated Raman scattering," Opt. Lett. **31**, 3480–3482 (2006).

1. Introduction

Over the past decade, tunable femtosecond laser systems with microjoule pulse energies in the visible spectral range have been developed based on three-wave mixing in nonlinear crystal [1-3]. Using noncollinear optical parametric amplifier (NOPA), these tunable femtosecond laser pulses have been widely used in pump-probe experiments [1-3]. Recently, interest in four-wave mixing (FWM) has been growing as an alternative [4-15]. Ultra-broadband spectra and ultrashort pulses have been generated in various optically transparent media using FWM [4-15]. Tunable, visible ultrashort pulses can be created using FWM by filamentation in a gas cell [6]. Few-cycle pulses in the deep UV and mid-IR have also been generated by this method [7, 8]. The energy conversion efficiency is low in a gas cell due to the small nonlinear coefficient. It was reported that high energy conversion efficiency FWM could be obtained in a gas filled hollow fiber owing to the long interaction distance [5]. In the case of solid-state media, phase matching can only be obtained when the pump beams cross at an angle due to the high material dispersion. By using ps pump pulses, high efficiency and high-energy noncollinear four-wave optical parametric amplification has been observed in a transparent bulk Kerr medium [9, 12]. Multicolor sidebands were generated in BK7 glass [4], in lead tungstate ($PbWO_4$) [10], in a BBO crystal [11], and in sapphire plate [14] using two crossed femtosecond laser beams.

In a recent work [15], tunable multicolor femtosecond laser pulses were generated simultaneously in a fused silica glass plate. These pulses can be used in many experiments, such as femtosecond CARS spectroscopy [16], two-dimensional spectroscopy [17], and some high intensity laser experiments [18] where two or more femtosecond pulses at different wavelengths are needed. However, the pulse energy of the sidebands was less than 200 nJ, limiting the applications in many fields.

In this letter, microjoule femtosecond pulses at different wavelengths are obtained by optimizing the spectrum and input power of one input beam and improving the spatial and temporal profile of the two input beams. Furthermore, the properties of output power, spectrum, exit angle, pulse duration, spatial profile and stability of the sidebands were studied. By changing the crossing angle on the glass plate, the wavelengths of the generated pulses can be tuned. The resulting sidebands can be used for multicolor pump-probe experiments as well as for spectrally and spatially mode entangled photon generation.

2. Experiment setup

A 1kHz Ti:sapphire regenerative amplifier femtosecond laser system (Micra+Legend-USP from Coherent) with 40-fs pulse duration and 2.5-W average power was used as the pump source. Following regenerative amplifier, the laser pulse was split into several beams. One of the beams (call it beam1) was spectrally broadened in a 60-cm hollow fiber with a 250-μm inner diameter filled with krypton gas. The broadband spectrum after the hollow fiber was dispersion compensated using a pair of chirped mirrors and a pair of glass wedges. The pulse duration after the hollow-fiber compressor was about 10 fs. After passing through a bandpass filter at 700 nm center wavelength with 40 nm bandwidth, beam1 was focused into a 1-mm-thick fused silica glass plate by a concave mirror. Another beam (called beam2) passed

#105514 - $15.00 USD Received 18 Dec 2008; revised 2 Feb 2009; accepted 23 Feb 2009; published 16 Mar 2009

through a delay stage having less than 3 fs resolution. Beam2 was first attenuated by a reflective variable neutral density (VND) filter and it was then focused into the fused silica glass plate by a lens. A third beam (beam3) was used to measure the pulse duration by the XFROG technique by mixing it with the two input beams or the generated sidebands in a 10-μm-thick BBO crystal.

The pulse durations of beam1 and beam2 were measured by XFROG with beam3 to be 40 ± 3 fs and 55 ± 3 fs, respectively, as shown in Fig. 1. The nearly equal pulse durations of the two input pulses demonstrates that they are temporally well overlapped. The retrieved wavelength dependent phase shows that beam2 has small positive chirp due to the dispersion of the beam splitters and lens. The spatial mode of the two input beams on the surface of the fused silica glass was measured using a CCD camera (BeamStar FX33 from Ophir Optronics), as shown in the inset of Fig. 1. The beam widths of beam2 were 500 μm and 300 μm in the horizontal and vertical directions, respectively. For beam1, the beam widths were 440 μm and 285 μm in the horizontal and vertical directions, respectively. These elliptical cross sections were obtained by adjusting the beams to the edges of the lens and concave mirror. Then the two beams were aligned to well overlap monitored by the CCD. Owing to their elliptic shapes, the two input beams can be made to overlap strongly in the medium even if there is a crossing angle between them. The glass was not damaged during the whole experiment because the intensity on the surface of the glass is one order lower than the optical breakdown threshold intensity of fused silica glass for femtosecond pulse.

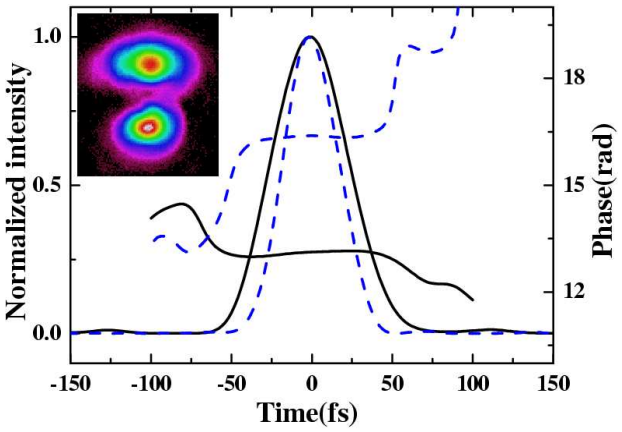

Fig. 1. The input pulse duration and phase of beam1 (dashed lines) and of beam2 (solid lines). The inset patterns are the two-dimensional beam profiles of beam1 (lower) and beam2 (upper) on the surface of the fused silica glass.

3. Experimental results and discussion

Multicolor cascaded FWM signals appeared individually in space beside the two input beams as beam1 and beam2 were synchronously on the fused silica glass in both time and space. The two input beams and the generated sidebands are horizontal polarization. The photograph at the top of Fig. 2(a) shows FWM sideband signals on a white sheet of paper placed about 30 cm after the glass plate. The input powers of beam1 and beam2 were 9 mW and 20 mW, respectively. An optical fiber was used to pick up different order signals to measure their spectra using a multichannel spectrometer (USB4000 from Ocean Optics). Figure 2(a) shows the spectra of the sideband wavelengths for the first-order Stokes (S1) through the fourth-order anti-Stokes (AS4) cascaded FWM signals along with the spectra of two input beams when the crossing angle between them was 1.87°. The spectrum extends from 450 to 1000 nm. The sidebands have a Gaussian profile and each anti-Stokes spectrum can support transform-limited pulse duration of about 25 fs. Moreover, the wavelengths of the sidebands can be tuned by changing the crossing angle between the two input beams. In this experiment,

#105514 - $15.00 USD Received 18 Dec 2008; revised 2 Feb 2009; accepted 23 Feb 2009; published 16 Mar 2009

beam2 was fixed and the crossing angle was changed by varying the position of beam1 on the surface of the concave mirror prior to the silica glass plate. Then there is about ± 0.02° error in every crossing angle. According to Fig. 2(b), the peak wavelength of AS3 can be tuned from 490 to 545 nm by changing the crossing angles from 1.40° to 2.57°. Compared with previous work [15], this tuning range is narrower, due to the narrower spectral bandwidth of beam2. A white screen was positioned 30 cm after the fused silica glass in order to mark the position of the sidebands for different crossing angles. In this way, the crossing angles between the generated sidebands and beam2 were recorded, as plotted in Fig. 3. The crossing angles between adjacent sidebands decreased as the order number increased for a given crossing angle between the input beams. Furthermore, the angle between each of the sidebands and beam2 increased with increasing of the crossing angle between the two input beams.

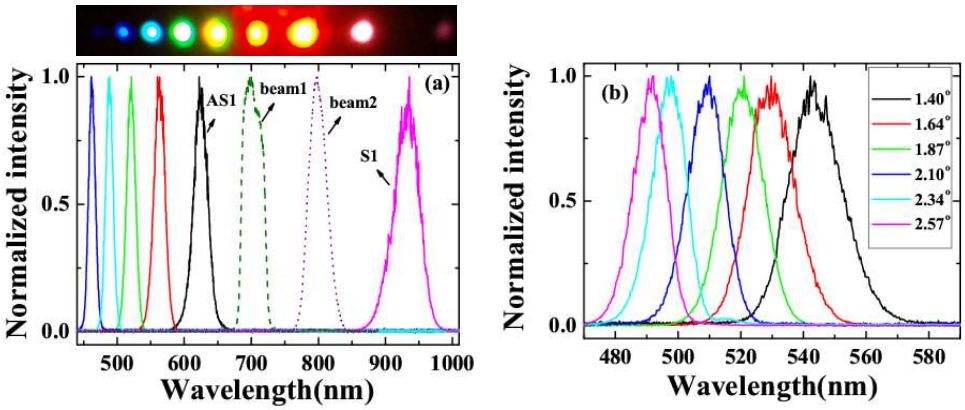

Fig. 2. (a) The spectra of the sidebands from S1 through AS5 and of the two input beams when the crossing angle between the two input beams was 1.87°. (b) Spectra of AS3 at crossing angles of 1.40°, 1.64°, 1.87°, 2.10°, 2.34°, and 2.57°. The photograph at the top of Fig. 2(a) shows the sidebands on a sheet of white paper placed 30 cm after the glass plate when the crossing angle between the two input beams was 1.87°. The first, second, and third spots from the right edge are S1, beam2, and beam1, respectively.

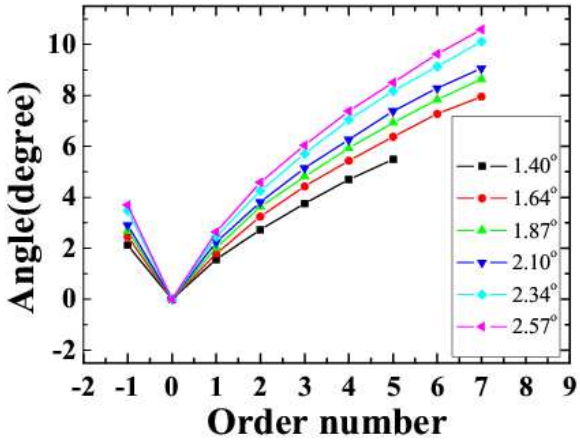

Fig. 3. Dependence of the angles between the generated sidebands and beam2 (with 0 order number) on the order number of the sidebands when the crossing angle between the two input beams was 1.40°, 1.64°, 1.87°, 2.10°, 2.34°, and 2.57°. Order number -1 refers to S1, 1 refers to AS1, and so on.

Regarding the cascaded FWM, the *m*-order sideband should obey the energy conservation and momentum conservation laws [4]: $(m+1)\omega_1-m\omega_2=\omega_{ASm}$ and $\boldsymbol{k}_{ASm}-(\boldsymbol{k}_1-\boldsymbol{k}_2)=\boldsymbol{k}_{AS(m-1)}$,

#105514 - $15.00 USD Received 18 Dec 2008; revised 2 Feb 2009; accepted 23 Feb 2009; published 16 Mar 2009

respectively. Here, 2 and 1 refer to the two input laser beams with $\omega_1 > \omega_2$. ASm refers to the generated m-order anti-Stokes sideband. As for *m*-order Stokes sideband, the energy conservation and momentum conservation laws are $(m+1)\omega_2 - m\omega_1 = \omega_{Sm}$ and $\boldsymbol{k}_{Sm} - (\boldsymbol{k}_2 - \boldsymbol{k}_1) = \boldsymbol{k}_{S(m-1)}$, respectively. Based on this phase matching condition, the best phase matching was achieved when the crossing angle was 1.9° in the experiment. This result accords with the output power shown in Fig. 4(a). In the simulation, this phase mismatching on the Stokes side is larger with the order number increasing. That is why there are less frequency down-shift sidebands than frequency up-shift signals. These results are the same as that of Ref. [4]. Simulation shows the tunable spectral range and the order number are limited by the phase matching condition [4]. In the experiment, both input pulses owe broader than 20nm spectrum. Therefore, the best phase matching condition can be achieved at different crossing angle when different frequency of the input pulses was taken part in the process. In this way, the spectrum of the sideband is tunable by changing the crossing angle [11]. The tunable spectral range is increased with the increasing of the order number.

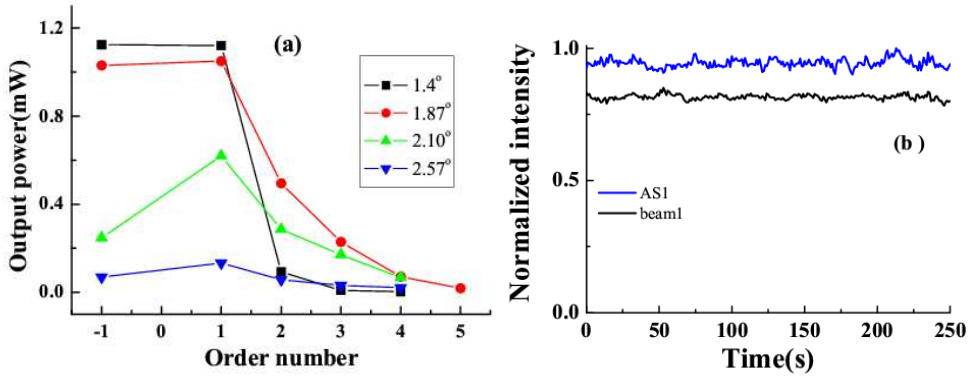

Fig. 4. (a) Dependence of the output power on the order number when the crossing angles between the two input beams were 1.40°, 1.87°, 2.10°, and 2.57°. Order number -1 refers to S1, 1 refers to AS1, and so on. (b) The stand deviations of AS1 and beam1, as monitored over four minutes, were 1.82% RMS and 0.97% RMS, respectively.

The output power of AS1 and S1 were 1.03 μJ and 1.05 μJ, respectively, when the crossing angle between the two input beams was 1.87° and the input powers of beam1 and beam2 were 9 mW and 20 mW, respectively. The output power of sidebands depends on the crossing angle between the two input beams and the order number of the sidebands. Figure 4(a) graphs the dependence of the output power on order number when the crossing angle between the two input beams was 1.40°, 1.87°, 2.10°, and 2.57°. The output power of S1 and AS1 decreased rapidly as the crossing angle between the two input beams increased from 1.40° to 2.57°. For a smaller crossing angle between the two input beams, say 1.40°, the output power of the sidebands decreased quickly with increasing order number. However, for a larger crossing angle between the two input beams, for example 2.57°, the output power of the sidebands slowly decreased as the order number increased. The energy conversion efficiency from the two input beams to sidebands was about 10% when the crossing angle between the two input beams was 1.87°. When the input power of beam2 was decreased to 15 mW, the output power of AS1 decreased to about 0.95 μJ. As the input power of beam2 increased to 30 mW, AS1 pulse energy as high as 1.15 μJ was obtained. Approximately the same power was obtained for 20-mW input power of beam2 when a 2-mm-thick fused silica glass plate was used. However, diffraction rings appeared around the output sidebands, reducing the beam quality seriously. When a 0.5-mm-thick fused silica glass was used as a medium, the output power of AS1 decreased to about 0.5 μJ. The output power of beam2 did not change at all during the cascade FWM process. The phenomenon indicates that the output power of the sidebands is

#105514 - $15.00 USD Received 18 Dec 2008; revised 2 Feb 2009; accepted 23 Feb 2009; published 16 Mar 2009

not sensitive to the input power of beam2, in agreement with the result of a previous work [15]. The power stability, as measured by the standard deviation of AS1 and beam1, was monitored over the course of four minutes, giving 1.82% RMS and 0.97% RMS, respectively, as shown in Fig. 4(b).

The pulse durations of S1, AS1, and AS2 were measured by generating cross-correlation signals with beam3. The XFROG trace was then retrieved using commercial software from Femtosoft Technologies. Figures 5(a) and 5(b) show the measured and retrieved traces of S1when the crossing angle was 1.87°. The corresponding traces of AS2 are shown in Figs. 5(c) and 5(d). The recovered intensity profiles and phases of AS1 and AS2 are depicted in Fig. 5(e) with retrieval errors of 0.011888 and 0.0097389, respectively. The pulse durations of AS1 and AS2 were thereby found to be 45 ± 3 fs and 44± 3 fs, respectively. Figure 5(f) shows the recovered pulse profile and phase of S1 with a retrieval error of 0.0049263. The pulse duration was 46± 3 fs. All of the generated sidebands have similar pulse duration. The retrieved phase shows that there was some chirp in the pulses due to the small positive chirp of the input pulses and the dispersion of the glass. Transform-limited sidebands may be obtained when the input pulses have a small negative chirp to compensate the dispersion of the glass.

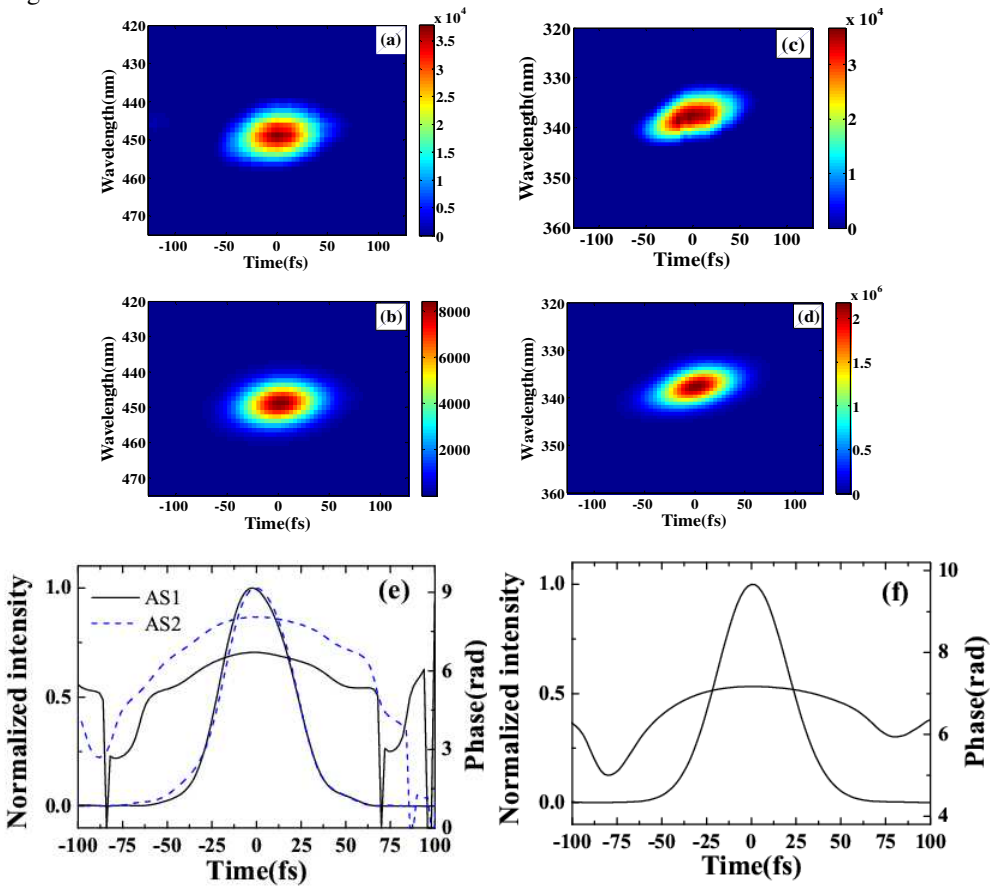

Fig. 5. (a) Measured and (b) retrieved XFROG traces of S1; (c) measured and (d) retrieved XFROG traces of AS2 when the crossing angle was 1.87°. (e) Recovered intensity profiles and phase of AS1 (solid line) and AS2 (dashed line) (f) Recovered pulse profile and phase of S1.

The spatial modes of the sidebands were measured using the CCD camera. All of the sidebands have Gaussian spatial profiles even though the input beams have elliptical cross sections. Figures 6(a) and 6(b) plot the two-dimensional spatial mode structure of S1 and

#105514 - $15.00 USD Received 18 Dec 2008; revised 2 Feb 2009; accepted 23 Feb 2009; published 16 Mar 2009

AS3, respectively. Figure 6(c) shows the one-dimension spatial profiles of S1 and AS3. A Gaussian fit curve to S1 is also shown in Fig. 6(c) and matches it well. The spot size of AS1 with a lens having a 700-mm focal length was measured to be less than 1.1 times the diffraction limit. Weak diffraction-like rings around AS1 and AS2 were observed on a white screen. Interestingly, beam2 was focused and its spatial mode changed from elliptic to circular in cross section during the process, accompanied by diffraction-like rings. Figures 6(d) and 6(e) show the two-dimensional spatial mode of beam2 when beam1 was blocked and when the input power of beam1 was 20 mW, respectively. The resulting spatial mode improvement may be due to the generation of multicolor solitons [19-20].

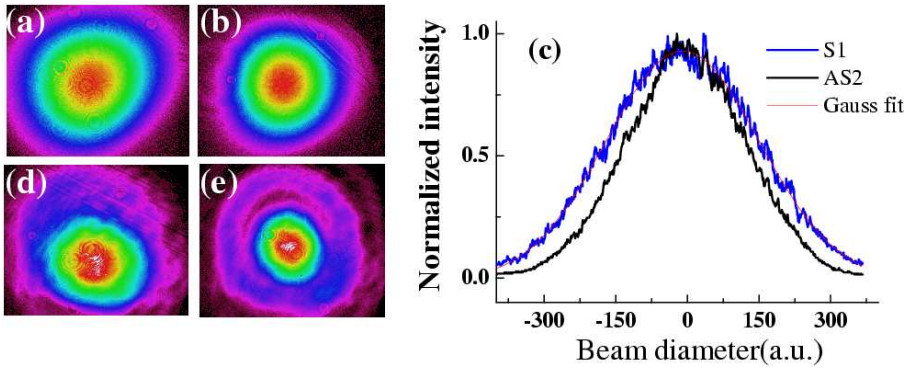

Fig. 6. The two-dimensional spatial modes of (a) S1 and (b) AS3. (c) The one-dimensional spatial profiles of S1 and AS3, together with a Gaussian fit to S1. The two-dimensional spatial mode of beam2 (d) when beam1 was blocked and (e) when the input power of beam1 was 20 mW.

4. Conclusion

In conclusion, frequency up-shift and down-shift microjoule multicolor femtosecond pulses were obtained at the same time by a cascaded FWM process in a fused silica glass plate. Approximately 45-fs laser pulse resulted at around 950nm. The energy conversion efficiency from the input beams to the sidebands was about 10%. The output powers, spectra, exit angles, pulse durations, spatial profiles and stabilities of the sidebands were studied. The properties of the generated sidebands will help people to choose the best parameters for various experiments, for example multicolor pump-probe experiment. In principle, there is no limitation to the output power as long as the input power is high enough owing to the size of the glass can be large enough.

Acknowledgment

We thank Zhiguang Wang for his technical assistance. This work was partly supported by the 21st Century COE program on “Coherent Optical Science” and partly supported by the grant from the Ministry of Education (MOE) in Taiwan under the ATU Program at National Chiao Tung University. A part of this work was performed under the joint research project of the Laser Engineering, Osaka University, under contract subject B1-27.

#105514 - $15.00 USD Received 18 Dec 2008; revised 2 Feb 2009; accepted 23 Feb 2009; published 16 Mar 2009